Chapter V

Applications

5.1 Introduction

In the last chapter, the form factors of the on-shell Z-penguin vertex function are computed numerically. In this chapter we shall apply our result to the following processes: (i) $s \to d Z^*$, (ii) $b \to s Z^*$ and (iii) $b \to d Z^*$, where Z^* is the virtual Z boson. The decay rates and decay rate asymmetry parameters will be computed as functions of the invariant mass k of Z^*. An analysis will also be performed on their dependence on the KM matrix elements. In the last section we shall also compute the decay rates and the decay asymmetries of the flavour-changing decays of Z^0 boson into $\bar{q}_1 q_2$ pair.

5.2 Decay Rates and Asymmetry Parameters for $q_1 \to q_2 Z^*$

From Chapter 3, the on-shell renormalized Z-penguin vertex function for the process $q_1 \to q_2 + Z^*$ is given by

$$\begin{aligned}\tilde{\Gamma}_{\mu,R}(\text{on-shell}) = \frac{gG_F}{4\sqrt{2}\pi^2 \cos\theta_w} \sum_j \lambda_j \Big\{ & (k_\mu \not{k} - k^2 \gamma_\mu)(A_j^L L + A_j^R R) \\ & + i\sigma_{\mu\nu} k^\nu (m_2 B_j^L L + m_1 B_j^R R) + M_w^2 (C_j^L \gamma_\mu L + C_j^R \gamma_\mu R) \Big\}\end{aligned} \tag{5.1}$$

which contain six form factors. Since $A_{jR} << A_{jL} (= A_j)$, $C_{jR} << C_{jR} (= C_j)$ and $B_{jR} \approx B_{jL}$ $(= B_j)$, we may rewrite Eq. (5.1) as

$$\begin{aligned}\tilde{\Gamma}_{\mu,R}(\text{on-shell}) = \frac{gG_F}{4\sqrt{2}\pi^2 \cos\theta_w} \sum_j \lambda_j \Big\{ & (k_\mu \not{k} - k^2 \gamma_\mu) A_j L \\ & + i\sigma_{\mu\nu} k^\nu (m_2 L + m_1 R) B_j + M_w^2 C_j \gamma_\mu L \Big\}\end{aligned} \tag{5.2}$$

Denoting $G \equiv \dfrac{gG_F}{4\sqrt{2}\pi^2 \cos\theta_w}$, the amplitude for the decay is

$$\mathcal{M}(q_1 \to q_2 Z^*) = G\sum_j \lambda_j \bar{u}_2 \Big\{ A_j \big(k_\mu \not{k} - k^2 \gamma_\mu\big) L + i\sigma_{\mu\nu} k^\nu B_j \big(m_1 R + m_2 L\big) M_W^2 C_j \gamma_\mu L \Big\} u_1 \varepsilon^\mu . \tag{5.3}$$

Here, u_1, u_2 are the spinors for the in-coming and out-going quarks respectively, whereas ε^μ is the polarization vector for the virtual Z boson. Because of the unitarity of the KM matrix, we have

$$\sum_j \lambda_j = 0. \tag{5.4}$$

One can then write

$$\sum_j \lambda_j F_j = \sum_j \lambda_j (F_j - F_t) \equiv \sum_j \lambda_j F_{jt}, \quad F = A, B \text{ or } C, \tag{5.5}$$

where we have defined

$$F_{jt} = F_j - F_t. \tag{5.6}$$

The decay rate is given by

$$\begin{aligned} \Gamma(q_1 \to q_2 Z^*) &= \frac{1}{m_1}\left(\frac{1}{4\pi}\right)^2 \frac{1}{2}\int \frac{|\mathcal{M}|^2}{E_2 E_k} \delta^4 \big(p_1 - p_2 - k\big) d^3 p_2 d^3 k \\ &= \frac{1}{2m_1}\int \frac{|\mathcal{M}|^2 |\boldsymbol{k}|^2}{4\pi E_2 E_k} \delta\left(m_1 - E_2 - E_k\right) d|\boldsymbol{k}| \\ &= \frac{1}{2m_1}\frac{|\mathcal{M}|^2}{4\pi E_2 E_k}\frac{|\boldsymbol{k}|^2}{d\big(E_2 + E_k\big)/d|\boldsymbol{k}|} \\ &= \frac{|\mathcal{M}|^2 |\boldsymbol{k}|}{8\pi m_1^2} \end{aligned} \tag{5.7}$$

where

$$\frac{d}{d|\boldsymbol{k}|}\left(E_2+E_k\right)=\frac{|\boldsymbol{k}|}{E_2}+\frac{|\boldsymbol{k}|}{E_Z} \tag{5.8}$$

and

$$m_1=E_2+E_k\,. \tag{5.9}$$

By conservation of energy-momentum of the virtual Z boson,

$$E_1=E_2+E_k \tag{5.10}$$

and

$$|\boldsymbol{k}|=|\boldsymbol{p}_2|\,, \tag{5.11}$$

and by the invariant mass squared of the virtual Z

$$k^2=E_k^2-|\boldsymbol{k}|^2\ , \tag{5.12}$$

we may find that $|\boldsymbol{k}|$ is related to the invariant mass squared as

$$|\boldsymbol{k}|^2=\frac{\left(k^2-m_1^2-m_2^2\right)^2}{4m_1^2}-m_2^2. \tag{5.13}$$

Therefore,

$$\Gamma(q_1\to q_2Z^*)=\frac{|\mathbb{M}_{\mathrm{L}}|^2}{8\pi m_1^2}\left[\frac{\left(k^2-m_1^2-m_2^2\right)^2}{4m_1^2}-m_2^2\right]^{\frac{1}{2}}. \tag{5.14}$$

Putting in Eq. (5.3) for the amplitude, and using Eq. (5.5), we arrive at

$$\begin{aligned}\Gamma\left(q_1\to q_2Z^*\right)\ =&\frac{1}{4\pi m_1^2}\left[\frac{\left(k^2-m_1^2-m_2^2\right)^2}{4m_1^2}-m_2^2\right]^{\frac{1}{2}}\frac{G^2}{2}\sum_{JJ'}\lambda_J\lambda_{J'}^*\left(-g^{\mu\mu'}+\frac{k^\mu k^{\mu'}}{M_Z^2}\right)\times\\ &\times Tr\Big\{\left(\not{p}_2+m_2\right)\Big\{\Big[A_{J\mu}\left(k_\mu k_\nu-k^2g_{\mu\nu}\right)+M_W^2C_{J\mu}g_{\mu\nu}\Big]\gamma^\nu L\\ &\quad+ik^\nu B_{J\mu}\sigma_{\mu\nu}\left(m_2L+m_1R\right)\Big\}\times\\ &\times\left(\not{p}_1+m_1\right)\Big\{\Big[A_{J'\nu}^*\left(k_{\mu'}k_{\nu'}-k^2g_{\mu'\nu'}\right)+M_W^2C_{J'\nu}^*g_{\mu'\nu'}\Big]\gamma^{\nu'}L\\ &\quad-ik^{\nu'}B_{J'\nu}^*\sigma_{\mu'\nu'}\left(m_1L+m_2R\right)\Big\}\Big\}\end{aligned} \tag{5.15}$$

$$
\begin{aligned}
&= \frac{1}{4\pi m_1^2}\left[\frac{\left(k^2 - m_1^2 - m_2^2\right)^2}{4m_1^2} - m_2^2\right]^{\frac{1}{2}} \frac{G^2}{2} \times \\
&\times \sum_{JJ'} \lambda_J \lambda_{J'}^* \left(-g^{\mu\mu'} + \frac{k^\mu k^{\mu'}}{M_Z^2}\right) Tr\{(\text{cross term}) \\
&\quad + \left[A_{J\mu}\left(k_\mu k_\nu - k^2 g_{\mu\nu}\right) + M_W^2 C_{J\mu} g_{\mu\nu}\right] \times \\
&\quad \times \left[A_{J'\mu}^*\left(k_{\mu'} k_{\nu'} - k^2 g_{\mu'\nu'}\right) + M_W^2 C_{J'\mu}^* g_{\mu'\nu'}\right]\left(\not{p}_2 \gamma^\nu \not{p}_1 \gamma^{\nu'} L\right) \\
&\quad - k^\nu B_{J\mu} k^{\nu'} B_{J'\mu}^* \left[\left(\not{p}_2 + m_2\right) i\sigma_{\mu\nu}\left(m_2 L + m_1 R\right) \times\right. \\
&\quad \left.\times \left(\not{p}_1 + m_1\right) i\sigma_{\mu'\nu'}\left(m_1 L + m_2 R\right)\right]\}
\end{aligned}
\tag{5.16}
$$

where

$$
\begin{aligned}
Tr(\text{cross term}) &= Tr\left\{-\left(\not{p}_2 + m_2\right)\left[A_{J\mu}\left(k_\mu k_\nu - k^2 g_{\mu\nu}\right) + M_W^2 C_{J\mu} g_{\mu\nu}\right] \times \right. \\
&\quad \times \left[\gamma^\nu L\left(\not{p}_1 + m_1\right) k^{\nu'} B_{J'\mu}^* i\sigma_{\mu'\nu'}\left(m_1 L + m_2 R\right)\right] \\
&\quad + \left(\not{p}_2 + m_2\right) k^\nu B_{J\mu} i\sigma_{\mu\nu}\left(m_2 L + m_1 R\right)\left(\not{p}_1 + m_1\right) \times \\
&\quad \left. \times \left[A_{J'\mu}^*\left(k_{\mu'} k_{\nu'} - k^2 g_{\mu'\nu'}\right) + M_W^2 C_{J'\mu}^* g_{\mu'\nu'}\right]\gamma^{\nu'} L\right\} \\
&= \frac{1}{2} Tr\left\{\left[A_{J\mu}\left(k_\mu k_\nu - k^2 g_{\mu\nu}\right) + M_W^2 C_{J\mu} g_{\mu\nu}\right] k^{\nu'} B_{J'\mu}^* \times \right. \\
&\quad \times \left(m_1^2 \not{p}_2 \gamma^\nu L + m_2^2 \gamma^\nu \not{p}_1 R\right)\left(\gamma^{\mu'} \gamma^{\nu'} - \gamma^{\nu'} \gamma^{\mu'}\right) \\
&\quad - \left[A_{J'\mu}^*\left(k_{\mu'} k_{\nu'} - k^2 g_{\mu'\nu'}\right) + M_W^2 C_{J'\mu}^* g_{\mu'\nu'}\right] k^\nu B_{J\mu} \times \\
&\quad \left. \times \left(m_1^2 \gamma^\nu \not{p}_2 R + m_2^2 \not{p}_1 \gamma^{\nu'} L\right)\left(\gamma^\mu \gamma^{\nu'} - \gamma^{\nu'} \gamma^\mu\right)\right\} .
\end{aligned}
\tag{5.17}
$$

In arriving at the expression for the decay rate in Eq. (5.15), we have averaged over all initial spin configurations and summed over the final spin configurations by manipulating the Dirac algebra as listed in the Appendix. After some the algebra, we obtain the following expression for the decay rate:

$$\Gamma(q_1 \to q_2 Z^*) = \frac{G^2}{4\pi m_1^2}\left[\frac{\left(k^2 - m_1^2 - m_2^2\right)^2}{4m_1^2} - m_2^2\right]^{\frac{1}{2}} \times$$
$$\times \sum_{jj'} \lambda_j \lambda_{j'}^* \left\{ f_1 A_{jl} A_{j'l}^* + f_2 B_{jl} B_{j'l}^* + f_3 C_{jl} C_{j'l}^* \right.$$
$$+ f_{12}\left(A_{jl} B_{j'l}^* + B_{jl} A_{j'l}^*\right) + f_{13}\left(A_{jl} C_{j'l}^* + C_{jl} A_{j'l}^*\right)$$
$$\left. + f_{23}\left(B_{jl} C_{j'l}^* + C_{jl} B_{j'l}^*\right)\right\} \tag{5.18}$$

where the f's are kinematic factors given by

$$f_1 = k^2\left(2k \cdot p_1 k \cdot p_2 + k^2 p_1 \cdot p_2\right) \tag{5.19a}$$

$$f_2 = \left(m_1^2 + m_2^2\right)\left(4k \cdot p_1 k \cdot p_2 - k^2 p_1 \cdot p_2\right) - 6m_1^2 m_2^2 k^2 \tag{5.19b}$$

$$f_3 = M_W^4\left[\left(2 - k^2 / M_Z^2\right)p_1 \cdot p_2 + 2k \cdot p_1 k \cdot p_2 / M_Z^2\right] \tag{5.19c}$$

$$f_{12} = -3k^2\left(m_1^2 k \cdot p_2 - m_2^2 k \cdot p_1\right) \tag{5.19d}$$

$$f_{13} = -M_W^2\left(2k \cdot p_1 k \cdot p_2 + k^2 p_1 \cdot p_2\right) \tag{5.19e}$$

$$f_{23} = 3M_W^2\left(m_1^2 k \cdot p_2 - m_2^2 k \cdot p_1\right). \tag{5.19f}$$

Similar calculation is performed for the charge-conjugated transition

$$\bar{q}_1 \to \bar{q}_2 + Z^*. \tag{5.20}$$

The corresponding on-shell renormalized vertex function is similar to that of Eq. (5.2) and is given by

$$\bar{\Gamma}_\mu(\bar{q}_1 \to \bar{q}_2 Z^*) = \frac{gG_F}{4\sqrt{2}\pi^2 \cos\theta_w} \sum_j \lambda_j \left\{ (k_\mu \not{k} - k^2 \gamma_\mu) A_j L \right.$$
$$\left. + i\sigma_{\mu\nu} k^\nu (m_1 L + m_2 R) B_j + M_w^2 C_j \gamma_\mu L \right\}. \tag{5.21}$$

The decay rate $\bar{\Gamma}$ for the charge-conjugated decay is then given by an expression similar to Γ in Eq. (5.17), but with $\lambda_j \lambda_{j'}^*$ replaced by $\lambda_j^* \lambda_{j'}$:

$$\overline{\Gamma}\left(\bar{q}_1 \to \bar{q}_2 Z^*\right) = \frac{G^2}{4\pi m_1^2}\left[\frac{\left(k^2 - m_1^2 - m_2^2\right)^2}{4m_1^2} - m_2^2\right]^{\frac{1}{2}} \times$$
$$\times \sum_{jl} \lambda_j^* \lambda_l \left\{ f_1 A_{jl} A_{jl}^* + f_2 B_{jl} B_{jl}^* + f_3 C_{jl} C_{jl}^* \right.$$
$$+ f_{12}\left(A_{jl} B_{jl}^* + B_{jl} A_{jl}^*\right) + f_{13}\left(A_{jl} C_{jl}^* + C_{jl} A_{jl}^*\right)$$
$$\left. + f_{23}\left(B_{jl} C_{jl}^* + C_{jl} B_{jl}^*\right)\right\}. \tag{5.22}$$

The asymmetry parameter a which is a measure of the direct CP violation effect is defined as

$$a = \frac{\left(\Gamma - \overline{\Gamma}\right)}{\left(\Gamma + \overline{\Gamma}\right)} = \frac{\Delta}{\Sigma}. \tag{5.23}$$

The expressions for Δ and Σ are given explicitly by

$$\Delta = \frac{G^2}{4\pi m_1^2}\left[\frac{\left(k^2 - m_1^2 - m_2^2\right)^2}{4m_1^2} - m_2^2\right]^{1/2} \times$$
$$\times \left[-2\,\mathrm{Im}\left(\lambda_u \lambda_c^*\right)\right]\left\{ f_1\,\mathrm{Im}\left(A_{ut} A_{ct}^*\right) + f_2\,\mathrm{Im}\left(B_{ut} B_{ct}^*\right) + f_3\,\mathrm{Im}\left(C_{ut} C_{ct}^*\right)\right. \tag{5.24}$$
$$+ f_{12}\,\mathrm{Im}\left(A_{ut} B_{ct}^* + B_{ut} A_{ct}^*\right) + f_{13}\,\mathrm{Im}\left(A_{ut} C_{ct}^* + C_{ut} A_{ct}^*\right) +$$
$$\left. + f_{22}\,\mathrm{Im}\left(B_{ut} C_{ct}^* + C_{ut} B_{ct}^*\right)\right\}$$

$$\Sigma = \frac{G^2}{4\pi m_1^2}\left[\frac{\left(k^2 - m_1^2 - m_2^2\right)^2}{4m_1^2} - m_2^2\right]^{1/2} \times$$
$$\times \left\{ \left|\lambda_u\right|^2 \left[f_1 \left|A_{ut}\right|^2 + f_2 \left|B_{ut}\right|^2 + f_3 \left|C_{ut}\right|^2 + f_{12}\,2\,\mathrm{Re}\left(A_{ut} B_{ut}^*\right)\right.\right.$$
$$\left. + f_{13}\,2\,\mathrm{Re}\left(A_{ut} C_{ut}^*\right) + f_{23}\,2\,\mathrm{Re}\left(B_{ut} C_{ut}^*\right)\right]$$
$$+ \left|\lambda_c\right|^2 \left[f_1 \left|A_{ct}\right|^2 + f_2 \left|B_{ct}\right|^2 + f_3 \left|C_{ct}\right|^2 + f_{12}\,2\,\mathrm{Re}\left(A_{ct} B_{ct}^*\right)\right.$$
$$\left. + f_{13}\,2\,\mathrm{Re}\left(A_{ct} C_{ct}^*\right) + f_{23}\,2\,\mathrm{Re}\left(B_{ct} C_{ct}^*\right)\right]$$
$$+ 2\,\mathrm{Re}\left(\lambda_u \lambda_c^*\right)\left[f_1\,\mathrm{Re}\left(A_{ut} A_{ct}^*\right) + f_2\,\mathrm{Re}\left(B_{ut} B_{ct}^*\right) + f_3\,\mathrm{Re}\left(C_{ut} C_{ct}^*\right)\right.$$
$$+ f_{12}\,\mathrm{Re}\left(A_{ut} B_{ct}^* + B_{ut} A_{ct}^*\right) + f_{13}\,\mathrm{Re}\left(A_{ut} C_{ct}^* + C_{ut} A_{ct}^*\right)$$
$$\left.\left. + f_{23}\,\mathrm{Re}\left(B_{ut} C_{ct}^* + C_{ut} B_{ct}^*\right)\right]\right\}. \tag{5.25}$$

The decay rates are

$$\Gamma(q_1 \to q_2 Z^*) = \frac{1}{2}(\Sigma + \Delta) \tag{5.26}$$

$$\overline{\Gamma}(\bar{q}_1 \to \bar{q}_2 Z^*) = \frac{1}{2}(\Sigma - \Delta). \tag{5.27}$$

For the decay of an in-coming quark (momentum p_1) into an out-going quark (momentum p_2) with an emission of a virtual Z boson (momentum k), conservation of energy-momentum requires

$$p_1 = p_2 + k. \tag{5.28}$$

Hence,

$$p_1 \cdot p_2 = \frac{1}{2}\left(m_1^2 + m_2^2 - k^2\right) \tag{5.29a}$$

$$k \cdot p_2 = \frac{1}{2}\left(m_1^2 - m_2^2 - k^2\right) \tag{5.29b}$$

$$k \cdot p_1 = \frac{1}{2}\left(m_1^2 - m_2^2 + k^2\right). \tag{5.29c}$$

The KM matrix elements enter Δ and Σ through the following combinations:

$$\left|\lambda_u\right|^2 = \left|V_{u2}V_{u1}\right|^2 \tag{5.30a}$$

$$\left|\lambda_c\right|^2 = \left|V_{c2}V_{c1}\right|^2 \tag{5.30b}$$

$$\mathrm{Re}\left(\lambda_u\lambda_c^*\right) = \mathrm{Re}\left(V_{u2}^*V_{u1}V_{c2}^*V_{c1}\right) \tag{5.30c}$$

$$J = \mathrm{Im}\left(\lambda_u\lambda_c^*\right) = \mathrm{Im}\left(V_{u2}^*V_{u1}V_{c2}^*V_{c1}\right). \tag{5.30d}$$

Here J is the invariant measure of CP violation [62]

$$J = 4.2^{+2.7}_{-1.4} \times 10^{-5}. \tag{5.31}$$

The following values for the relevant KM matrix elements will be used in the subsequent analysis: [63]

$$|V_{ud}| = 0.9744 \pm 0.0010 \tag{5.32a}$$

$$|V_{us}| = 0.2205 \pm 0.0018 \tag{5.32b}$$

$$|V_{cd}| = 0.204 \pm 0.017 \tag{5.32c}$$

$$|V_{cb}| = 0.040 \pm 0.005 \tag{5.32d}$$

$$|V_{cs}| = 0.9782 \pm 0.0036 \tag{5.32e}$$

$$|V_{ub}| = 0.0032 \pm 0.0009 . \tag{5.32f}$$

The analysis of the decay rates and asymmetry parameters for the process

$$s \to dZ^*$$

$$b \to sZ^*$$

$$b \to dZ^*$$

will be presented in the next section.

5.3 Analysis and Result of the Decay Rates and Asymmetry Parameters for $q_1 \to q_2 Z^*$

I. The process $s \to dZ^*$

The physical region for this process is given by $k^2 < (m_t - m_d)^2 = (0.19\text{GeV})^2$. The values for $|\lambda_u|^2$ and $|\lambda_t|^2$ are respectively

$$|\lambda_u|^2 = 0.0462 \pm 0.0008 \tag{5.33a}$$

$$|\lambda_t|^2 = 0.040 \pm 0.007. \tag{5.33b}$$

The value of $\text{Re}(\lambda_u \lambda_c^*)$ depends on the relative phases of the KM matrix elements involved. Since

$$\lambda_u + \lambda_c + \lambda_t = 0 \tag{5.34}$$

and

$$\lambda_t \approx 0, \tag{5.35}$$

we have

$$\lambda_u \approx -\lambda_c. \tag{5.36}$$

The relative phase between λ_c and λ_u is thus almost 180°. Using the values for $|\lambda_u|^2$ and $|\lambda_t|^2$ as given in Eq. (5.33), we obtain the following estimate for $\text{Re}(\lambda_u \lambda_c^*)$:

$$\begin{aligned} \text{Re}(\lambda_u \lambda_c^*) &= |\lambda_c||\lambda_u| \cos\phi \\ &= -\sqrt{|\lambda_u|^2 \, |\lambda_c|^2 - J^2} \\ &= -0.0430 \pm 0.0005 \end{aligned} \tag{5.37}$$

where the relative phase ϕ between λ_u and λ_c may be determined from

$$\text{Im}(\lambda_u \lambda_c^*) / \text{Re}(\lambda_u \lambda_c^*) = \tan\phi. \tag{5.38}$$

In the following analysis, $|\lambda_u|^2$, $|\lambda_c|^2$ and $\mathrm{Re}(\lambda_u\lambda_c^*)$ shall be fixed at 0.0462, 0.040 and -0.043 respectively. The variations of decay rate Γ and a with the invariant mass k of the virtual Z boson are displayed in Figs 5.1 and 5.2. Figs. 5.3 and 5.4 display the variations of Γ and a against $|\lambda_t|^2$ with k^2 fixed at $(0.1\mathrm{GeV})^2$, and $|\lambda_t|^2$ is allowed to vary from 0.03 to 0.05. In this analysis $\mathrm{Re}(\lambda_u\lambda_c^*)$ is made to be dependent on $|\lambda_t|^2$ through the relation

$$\begin{aligned}\mathrm{Re}(\lambda_u\lambda_c^*) &= |\lambda_u||\lambda_c|\cos\phi \\ &= -\sqrt{|\lambda_c|^2|\lambda_u|^2 - J^2}.\end{aligned} \tag{5.39}$$

From Fig. 5.1 we find that the decay rate is found to be very small, being in the order of 10^{-12} GeV. The factor of $|\mathrm{k}| = \sqrt{\left[(k^2 - m_1^2 - m_2^2)^2 / 4m_1^2 - m_2^2\right]}$ appeared in the expression for the decay rate in Eq. (5.14) suggests that the decay rate vanishes when k^2 approaches its largest allowed value. This limiting behaviour of the decay rate is vividly displayed in Fig. 5.1. From Fig. 5.2 we find that the asymmetry parameter a rise sharply from zero above the threshold for the u quark. Within the physical range of k, a range from $\sim -2\times10^{-7}$ to $\sim -7\times10^{-7}$.

Figs. 5.3 and 5.4 show interesting behaviour of very steep variations of Γ and a against $|\lambda_t|^2$. Fig. 5.3 show strong dependence of decay rate with respect to $|\lambda_t|^2$. Γ decreases sharply to a value of $\sim 5\times10^{-15}$ GeV at $|\lambda_t|^2 = 0.046$. We find that the decay rate ranges from $\sim 1\times10^{-11}$ to the minimum of $\sim 5\times10^{-15}$ GeV, where it varies for 4 orders in magnitude. In Fig. 5.4, the value of a sharply peaks at the value of $|\lambda_t|^2$ at around 0.046 to reach a magnitude of $\sim 4\times10^{-4}$. Whereas at other values of $|\lambda_t|^2$, a is much smaller in magnitude. Within the range of variation of $|\lambda_t|^2$, a may vary as much as 4 orders in

magnitude. The sharp decrease in Γ at $|\lambda_c|^2 = 0.046$ explains the sharp increases in a at the same value of $|\lambda_c|^2$.

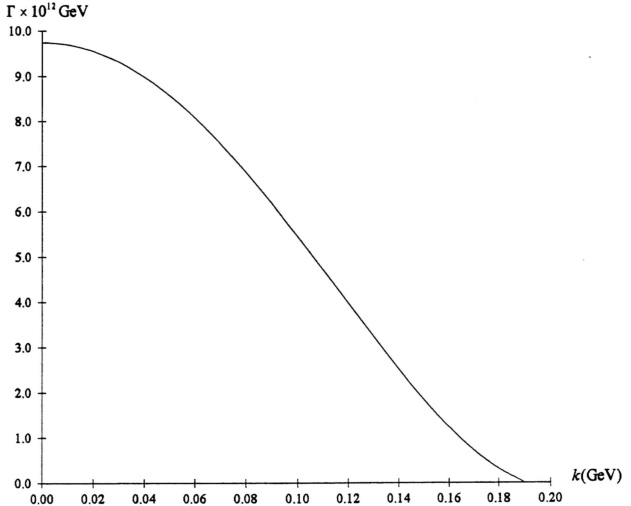

Figure 5.1. Decay rate Γ versus invariant mass invariant mass k of the virtual Z boson for $s \rightarrow d Z^{*}$.

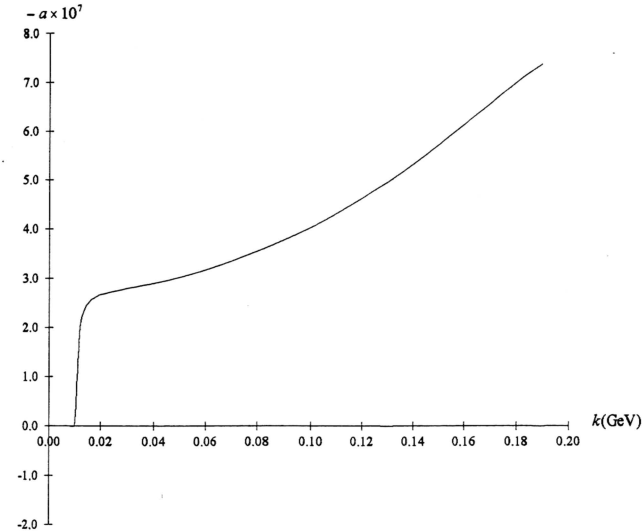

Figure 5.2. Asymmetry parameter a versus invariant mass k of the virtual Z boson for $s \rightarrow d Z^*$.

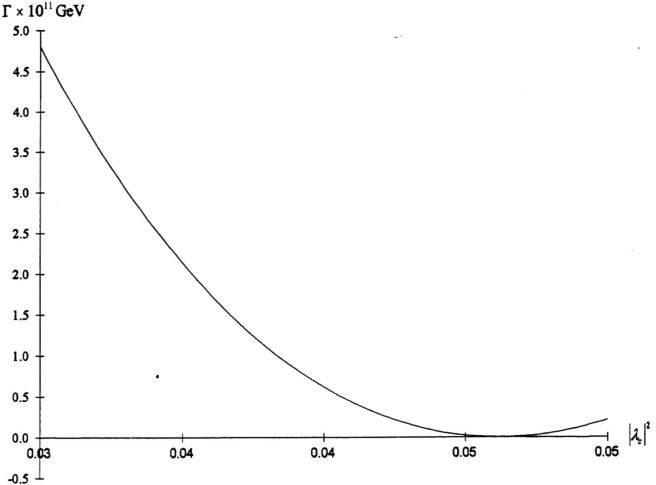

Figure 5.3. Decay rate Γ versus $|\lambda_c|^2$ for $s \to d Z^*$ at $k^2 = (0.1\text{GeV})^2$.

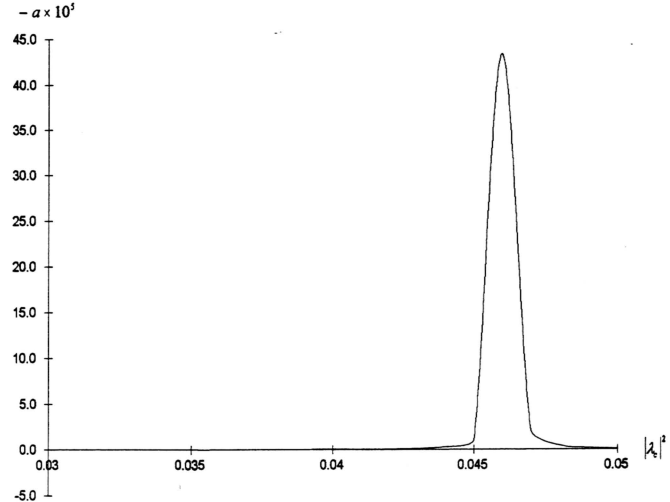

Figure 5.4. Asymmetry parameter a versus $|\lambda_e|^2$ for $s \to d Z^*$ at $k^2 = (0.1\text{GeV})^2$.

II. The process $b \to sZ^*$

The physical region for this process is given by $0 < k^2 < (m_b - m_s)^2 = (4.1\text{GeV})^2$. The values for $|\lambda_u|^2$ and $|\lambda_t|^2$ are :

$$|\lambda_u|^2 = (5 \pm 3) \times 10^{-7} \tag{5.40a}$$

$$|\lambda_t|^2 = 0.00153 \pm 0.00004. \tag{5.40b}$$

We shall neglect $|\lambda_u|^2$ compared with $|\lambda_t|^2$. Since $|\text{Re}(\lambda_u \lambda_c^*)| < |\lambda_u||\lambda_t|$, we shall also ignore $|\text{Re}(\lambda_u \lambda_c^*)|$. Hence only $|\lambda_t|^2$ is dominant.

Figs. 5.5 and 5.6 show the variations of decay rate Γ and a with respect to k. A similar behaviour to the corresponding transition of $s \to dZ^*$ is observed. But in this case there are two thresholds, namely $k^2 = (2m_u)^2$ and $k^2 = (2m_c)^2$, that are within the physical range of k. From Fig. 5.5, the decay rate Γ is of order $\sim 10^{-9}$ GeV and behave similarly as in $s \to dZ^*$, where it tends to zero when k approaching its upper physical limit. In Fig. 5.6, we observe that a rises abruptly from zero when k passes through the threshold at $k^2 = (2m_u)^2$. Magnitude of a increases slowly between $\sim 1.6 \times 10^{-5}$ to $\sim 2.8 \times 10^{-5}$ as k varies from $k^2 = (2m_u)^2$ until it reaches another threshold at $k^2 = (2m_c)^2$, after which it drops steeply due to the on-set of the contribution form the imaginary form factors for internal quark c. The overall magnitude for a is of the order $\sim 10^{-5}$. Compared to $s \to dZ^*$, the magnitude of a is smaller because the decay rate is higher.

The variations of a and Γ with respect to KM matrix elements is not analysed here since the dependence is expected to be very slight.

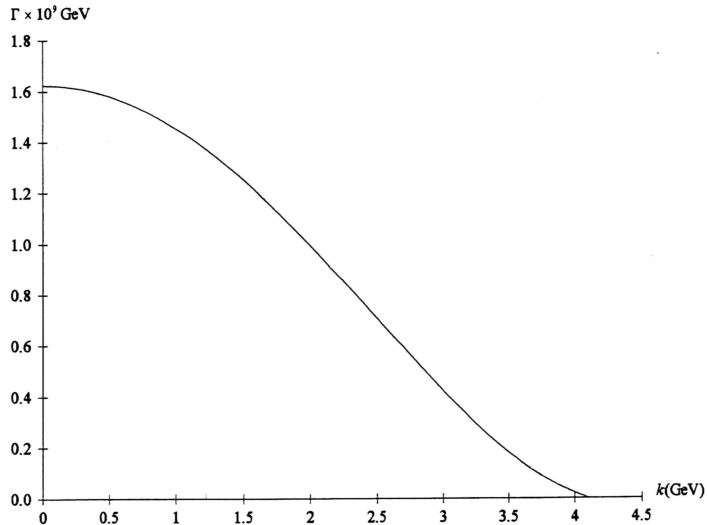

Figure 5.5. Decay rate Γ versus invariant mass k of the virtual Z boson for $b \to s Z^*$.

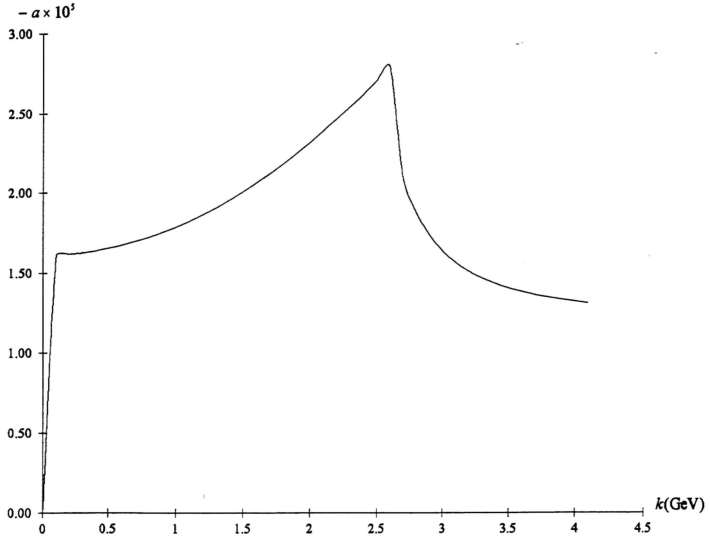

Figure 5.6. Asymmetry parameter a versus invariant mass k of the virtual Z boson for $b \to s Z^*$.

III. The process $b \to dZ^*$

The physical region for this process is $k^2 < (m_b - m_d)^2 = (4.29\text{GeV})^2$. The values for $|\lambda_u|^2$ and $|\lambda_c|^2$ are

$$|\lambda_u|^2 = (9.72 \pm 5.49) \times 10^{-6} \tag{5.41a}$$

$$|\lambda_c|^2 = (6.66 \pm 2.77) \times 10^{-5}. \tag{5.41b}$$

Due to the large error associated with the KM matrix elements for $b \to d$ transition, we can not determine, with the same certainty as in the case of $s \to d$ transition, the phase between λ_u and λ_c. We shall therefore take the value of $\text{Re}(\lambda_u \lambda_c^*)$ to fall within the following range:

$$-|\lambda_u||\lambda_c| < \text{Re}(\lambda_u \lambda_c^*) < |\lambda_u||\lambda_c|. \tag{5.42}$$

In the following analysis, $|\lambda_u|^2$ is fixed at 9.72×10^{-6}.

The variations of Γ and a with the invariant mass k of the virtual Z boson are displayed in Figs. 5.7 and 5.8 for the two extreme values of $\text{Re}(\lambda_u \lambda_c^*)$ of $\pm 2.54 \times 10^{-5}$ while fixing $|\lambda_t|^2$ at 6.66×10^{-5}.

Figs. 5.9 and 5.10 show the variations of decay rate and a with $|\lambda_t|^2$ for the two extreme values of $\text{Re}(\lambda_u \lambda_c^*) = \pm |\lambda_u||\lambda_c|$ while $|\lambda_t|^2$ is allowed to vary from 3×10^{-5} to 10×10^{-5} with fixed $k^2 = (2.0\,\text{GeV})^2$. In this case, $\text{Re}(\lambda_u \lambda_c^*)$ is taken to be $\text{Re}(\lambda_u \lambda_c^*) = \pm |\lambda_u||\lambda_c|$.

We also vary the decay rate and asymmetry parameter with respect to $\text{Re}(\lambda_u \lambda_c^*)$ which we set to range from -2.6×10^{-5} to 2.6×10^{-5}. Figs. 5.11 and Fig. 5.12 show variations of Γ and a with $\text{Re}(\lambda_u \lambda_c^*)$ at $|\lambda_t|^2 = 6.66 \times 10^{-5}$ and $k^2 = (2.0\,\text{GeV})^2$.

From Fig. 5.7, the decay rate for $\mathrm{Re}(\lambda_u \lambda_c^*) = -2.54 \times 10^{-5}$ is generally smaller in magnitude and is of order $\sim 10^{-11}$ GeV, they also show limiting behaviour to zero as k tends to its upper physical limit. Whereas from Fig. 5.8, we observe that a is of order $\sim 10^{-4}$ and magnitude of a for $\mathrm{Re}(\lambda_u \lambda_c^*) = -2.54 \times 10^{-5}$ is generally larger and it shows similar threshold behaviour as in the case of $b \to s Z^*$.

For both Γ and a, their dependence on $|\lambda_t|^2$, as well as on $\mathrm{Re}(\lambda_u \lambda_c^*)$, is slight, as shown in Figs. 5.9 to 5.12.

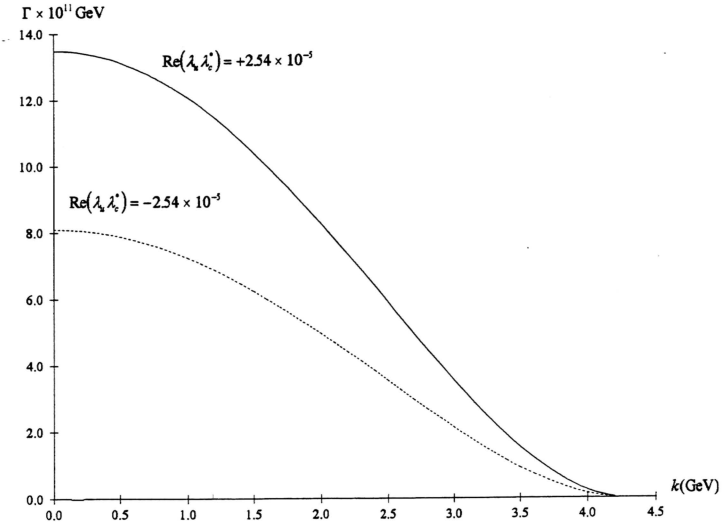

Figure 5.7. Decay rate Γ versus invariant mass k of the virtual Z boson for $b \to d\,Z^*$.

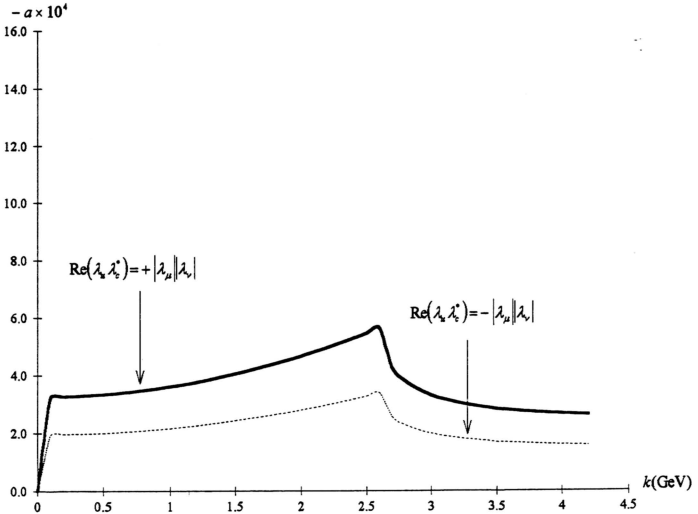

Figure 5.8. Asymmetry parameter a versus invariant mass k of the virtual Z boson for $b \to d\, Z^*$.

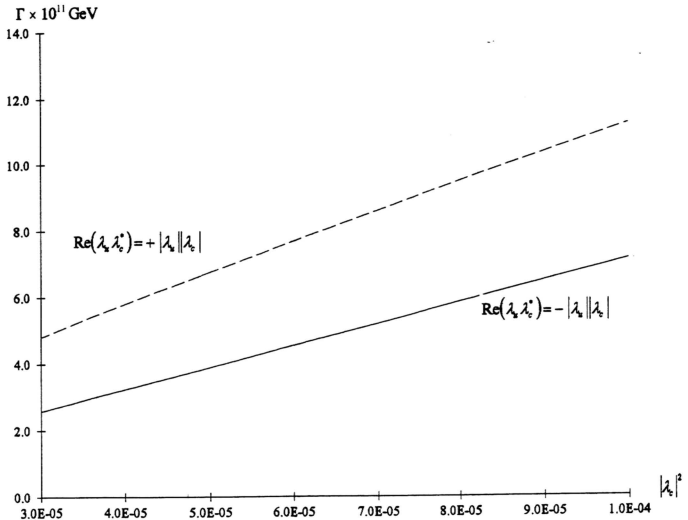

Figure 5.9. Decay rate Γ versus $|\lambda_c|^2$ for $b \to d Z^*$ at $k^2 = (2.0\text{GeV})^2$.

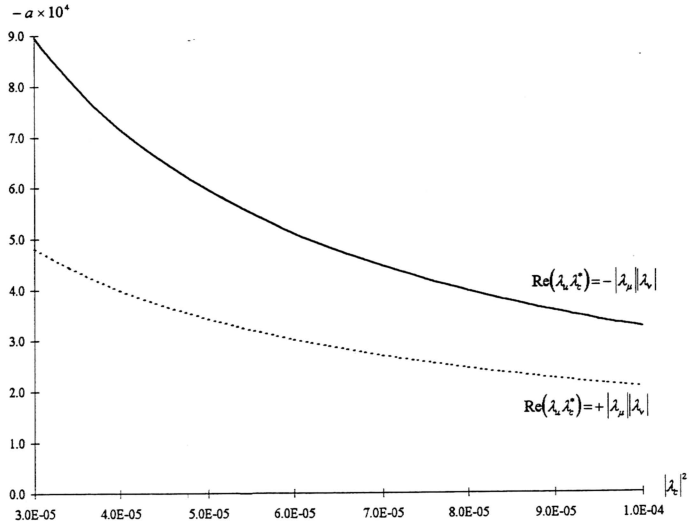

Figure 5.10. Asymmetry parameter a versus $|\lambda_c|^2$ for $b \to d Z^*$ at $k^2 = (2.0\mathrm{GeV})^2$.

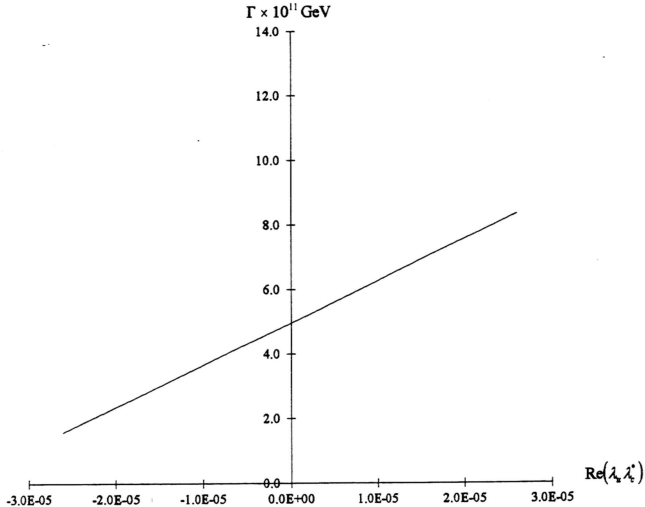

Figure 5.11. Decay rate Γ versus $\mathrm{Re}(\lambda_s \lambda_t^*)$ for $b \to d Z^*$ at $k^2 = (2.0\mathrm{GeV})^2$.

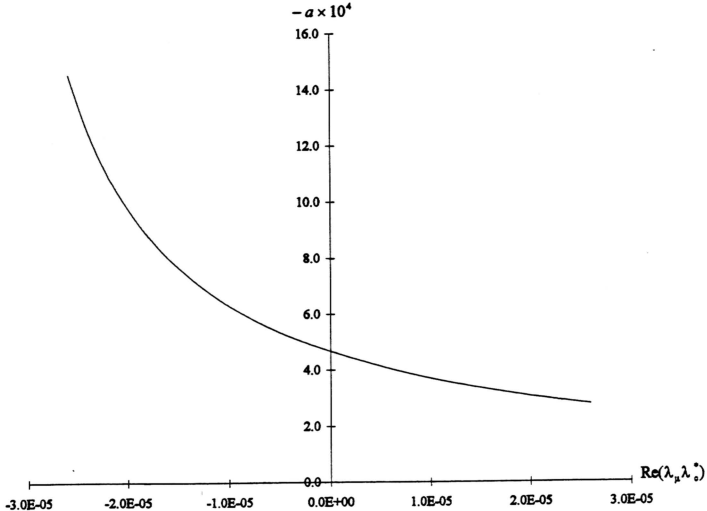

Figure 5.12. Asymmetry parameter a versus $\mathrm{Re}(\lambda_u \lambda_c^*)$ for $b \to d Z^*$ at $k^2 = (2.0\mathrm{GeV})^2$.

Two key ingredients are important for direct *CP* violation to come into play in the processes considered, namely (i) the complexity of KM elements, which is exemplified by the invariant measure of *CP*, $J = \mathrm{Im}(\lambda_u \lambda_c^*)$, and (ii) the development of absorptive parts in the vertex function form factors, which arises whenever $k^2 > 4m_j^2$, for $j = u$, c or t.

The asymmetry parameter a displays the following general behaviour as k increases. Its magnitude $|a|$ rises from zero sharply above $k = 0.01$ GeV, corresponding to the threshold for the internal u quark. It then decreases rapidly after the threshold for the c quark at $k = 2.6$ GeV, if it is within the physical region. The t quark threshold at $k = 352$ GeV is however too far away from the physical region. There is another threshold at $k = 2M_w$, which is outside the physical region for all the processes considered here.

The kinematic factors also play an important role in determining the magnitude of a. Since f_3 is much larger than the other kinematic factors, it is expected that the f_3 term in Σ is the dominant term. This is however not true for Δ, because the imaginary parts of the form factors come into active play. For the transition $b \to sZ^*$, f_3 is larger than f_{13} and f_{23} by a factors $M_W^2 / m_b^2 \sim 2.6 \times 10^2$. But at the same time, $\mathrm{Im}\, A_u$ and $\mathrm{Im}\, A_c$ are larger than $\mathrm{Im}\, C_u$ and $\mathrm{Im}\, C_c$ by a factor larger than this. Thus the A_j form factors are as important as the C_j form factors for the asymmetry parameter in $b \to sZ^*$, which is of the order 10^{-5}. For the decay $s \to dZ^*$, since $M_W^2 / m_s^2 \sim 1.5 \times 10^5$, only the C_j form factors are important, and the asymmetry parameter is of order 10^{-7}. The asymmetry parameter for $b \to dZ^*$ transition is roughly of the order of 10^{-4}. Generally the asymmetry parameter is larger for the process with smaller decay rate.

Interesting variations of asymmetry parameters and decay rates with KM matrix elements $|\lambda_t|^2$ and $\mathrm{Re}(\lambda_u \lambda_c^*)$ are also displayed. We see that the value of the decay

asymmetries and decay rates may have certain dependence on the variation of these KM matrix elements. The most prominent example is in the $s \to d$ transition where Γ and a vary as much as 4 orders in magnitude, as $|\lambda_t|^2$ varies within the experimental range. When the decay rate drops to a minimum at $|\lambda_t|^2 \sim 0.046$, the corresponding a reaches a maximum and peaks sharply.

Whereas in the $b \to d$ transition the dependence on $|\lambda_t|^2$ is rather flat. The variation with respect to $\mathrm{Re}(\lambda_u \lambda_c^*)$ is at an order in magnitude the most. The value of $|a|$ is generally about two to five times higher than that for $\mathrm{Re}(\lambda_u \lambda_c^*) = 2.54 \times 10^{-5}$, whereas the decay rate is generally a few times higher than the value for that of $\mathrm{Re}(\lambda_u \lambda_c^*) = -2.54 \times 10^{-5}$.

The decay rates for $s \to d Z^*$, $b \to s Z^*$ and $b \to d Z^*$ are of the order 10^{-12}, 10^{-9} and 10^{-11} GeV respectively.

Finally, the importance of the A_j form factors need to be emphasised. For the decay $q_1 \to q_2 Z^*$, $\mathrm{Im} A_{u,c}$ is considerably larger than $\mathrm{Im} C_{u,c}$ so as to overcome kinematic suppression. Hence A_j form factors are as important as C_j in contributing to the asymmetry parameter of such decays.

5.4 Flavour Changing Decay of $Z^0 \to q_2\bar{q}_1$

In this section we shall apply $Zq_1\bar{q}_2$ vertex to the flavour-changing decay of Z^0 boson: $Z^0 \to \bar{q}_1 q_2, \bar{q}_2 q_1$.[34,49,50] The form factors for the above process is obtained by setting $k^2 = M_Z^2$, and they are displayed in Table 5.1. The mass of the Z boson is taken to be 91.19 GeV.

Table 5.10. Form Factors for $Zq_1\bar{q}_2$ vertex at $k^2 = M_Z^2$.

	Internal quark		
	u	c	t
Re A	-3.6212×10^{-1}	-3.6227×10^{-1}	1.6986×10^{-1}
Re B	-6.3327×10^{-2}	-6.3309×10^{-2}	2.7415×10^{-1}
Re C	-0.4511	-4.5079×10^{-1}	2.9891
Im A	5.6687×10^{-1}	5.6693×10^{-1}	0
Im B	1.1122×10^{-1}	1.1115×10^{-1}	0
Im C	1.0232×10^{-8}	6.9145×10^{-4}	0

The calculation for Z^0 decay is slightly different from the case of $q_1 \to q_2 Z^*$. The vertex function for Z^0 decay is given by

$$\begin{aligned}\tilde{\Gamma}^{\alpha}_{\mu,R}(Z^0 \to \bar{q}_1 q_2) = \frac{gG_F}{4\sqrt{2}\pi^2\cos\theta_w}\sum_j \lambda_j \Big\{ &(k_\mu \not{k} - k^2\gamma_\mu)A_j L \\ &+ i\sigma_{\mu\nu}k^\nu(m_2 L + m_1 R)B_j + M_w^2 C_j \gamma_\mu L\Big\}.\end{aligned} \tag{5.43}$$

Proceeding as in Section 5.1, we obtain the following expression for the decay rate,

$$\Gamma\left(Z^0 \to \bar{q}_1 q_2\right) = \frac{G^2}{8\pi M_z} \sum_{jj'} \lambda_j \lambda_{j'}^* \left\{ \tilde{f}_1 A_{jl} A_{j'l}^* + \tilde{f}_2 B_{jl} B_{j'l}^* + \tilde{f}_3 C_{jl} C_{j'l}^* + \tilde{f}_{12}\left(A_{jl} B_{j'l}^* + B_{jl} A_{j'l}^*\right) + \tilde{f}_{13}\left(A_{jl} C_{j'l}^* + C_{jl} A_{j'l}^*\right) + \tilde{f}_{23}\left(B_{jl} C_{j'l}^* + C_{jl} B_{j'l}^*\right) \right\}, \tag{5.44}$$

where the kinematic factors are given by

$$\tilde{f}_1 = f_1 = k^2\left(2k \cdot p_1 k \cdot p_2 + k^2 p_1 \cdot p_2\right) \tag{5.45a}$$

$$\tilde{f}_2 = \left(m_1^2 + m_2^2\right)\left(4k \cdot p_1 k \cdot p_2 - k^2 p_1 \cdot p_2\right) + 6m_1^2 m_2^2 k^2 \tag{5.45b}$$

$$\tilde{f}_3 = f_3 = M_W^4\left[\left(2 - k^2 / M_z^2\right) p_1 \cdot p_2 + 2k \cdot p_1 k \cdot p_2 / M_z^2\right] \tag{5.45c}$$

$$\tilde{f}_{12} = -3k^2\left(m_1^2 k \cdot p_2 + m_2^2 k \cdot p_1\right) \tag{5.45d}$$

$$\tilde{f}_{13} = f_{13} = -M_W^2\left(2k \cdot p_1 k \cdot p_2 + k^2 p_1 \cdot p_2\right) \tag{5.45e}$$

$$\tilde{f}_{23} = 3M_W^2\left(m_1^2 k \cdot p_2 + m_2^2 k \cdot p_1\right). \tag{5.45f}$$

To obtain the decay rate asymmetry a, we note that the vertex function for the decay $Z^0 \to q_1 \bar{q}_2$ is given by

$$\tilde{\Gamma}_{\mu,R}(Z^0 \to q_1 \bar{q}_2) = \frac{gG_F}{4\sqrt{2}\pi^2 \cos\theta_w} \sum_j \lambda_j \left\{ (k_\mu \not{k} - k^2 \gamma_\mu) A_j L - i\sigma_{\mu\nu} k^\nu (m_1 L + m_2 R) B_j + M_w^2 C_j \gamma_\mu L \right\} \tag{5.46}$$

which gives the following expression for the corresponding decay rate:

$$\Gamma\left(Z^0 \to q_1 \bar{q}_2\right) = \frac{G^2}{8\pi M_z} \sum_{jj'} \lambda_j^* \lambda_{j'} \left\{ \tilde{f}_1 A_{jl} A_{j'l}^* + \tilde{f}_2 B_{jl} B_{j'l}^* + \tilde{f}_3 C_{jl} C_{j'l}^* + \tilde{f}_{12}\left(A_{jl} B_{j'l}^* + B_{jl} A_{j'l}^*\right) + \tilde{f}_{13}\left(A_{jl} C_{j'l}^* + C_{jl} A_{j'l}^*\right) + \tilde{f}_{23}\left(B_{jl} C_{j'l}^* + C_{jl} B_{j'l}^*\right) \right\} \tag{5.47}$$

The asymmetry a is then easily computed and is given by essentially the same expression as in Eq. (5.23):

$$a = \Delta / \Sigma \tag{5.48}$$

$$\begin{aligned}\Delta = \frac{G^2}{8\pi M_Z}\Big[-2\,\mathrm{Im}\big(\lambda_u \lambda_c^*\big)\Big]\Big\{& f_1\,\mathrm{Im}\big(A_{ut}A_{ct}^*\big) + f_2\,\mathrm{Im}\big(B_{ut}B_{ct}^*\big) + f_3\,\mathrm{Im}\big(C_{ut}C_{ct}^*\big) \\ & + f_{12}\,\mathrm{Im}\big(A_{ut}B_{ct}^* + B_{ut}A_{ct}^*\big) + f_{13}\,\mathrm{Im}\big(A_{ut}C_{ct}^* + C_{ut}A_{ct}^*\big) + \\ & + f_{22}\,\mathrm{Im}\big(B_{ut}C_{ct}^* + C_{ut}B_{ct}^*\big)\Big\}\end{aligned} \tag{5.49}$$

and

$$\begin{aligned}\Sigma = \frac{G^2}{8\pi M_Z}\Big\{& |\lambda_u|^2\Big[f_1|A_{ut}|^2 + f_2|B_{ut}|^2 + f_3|C_{ut}|^2 + f_{12}\,2\,\mathrm{Re}\big(A_{ut}B_{ut}^*\big) \\ & + f_{13}\,2\,\mathrm{Re}\big(A_{ut}C_{ut}^*\big) + f_{23}\,2\,\mathrm{Re}\big(B_{ut}C_{ut}^*\big)\Big] \\ & + |\lambda_c|^2\Big[f_1|A_{ct}|^2 + f_2|B_{ct}|^2 + f_3|C_{ct}|^2 + f_{12}\,2\,\mathrm{Re}\big(A_{ct}B_{ct}^*\big) \\ & + f_{13}\,2\,\mathrm{Re}\big(A_{ct}C_{ct}^*\big) + f_{23}\,2\,\mathrm{Re}\big(B_{ct}C_{ct}^*\big)\Big] \\ & + 2\,\mathrm{Re}\big(\lambda_u\lambda_c^*\big)\Big[f_1\,\mathrm{Re}\big(A_{ut}A_{ct}^*\big) + f_2\,\mathrm{Re}\big(B_{ut}B_{ct}^*\big) + f_3\,\mathrm{Re}\big(C_{ut}C_{ct}^*\big) \\ & + f_{12}\,\mathrm{Re}\big(A_{ut}B_{ct}^* + B_{ut}A_{ct}^*\big) + f_{13}\,\mathrm{Re}\big(A_{ut}C_{ct}^* + C_{ut}A_{ct}^*\big) \\ & + f_{23}\,\mathrm{Re}\big(B_{ut}C_{ct}^* + C_{ut}B_{ct}^*\big)\Big]\Big\}.\end{aligned} \tag{5.50}$$

The analysis of the decay rates and asymmetry parameters for the processes $Z^0 \to s\bar{d},\ b\bar{s},\ b\bar{d}$ will be presented separately in the following.

I. The process $Z^0 \to d\bar{s}, s\bar{d}$

The variations of decay rate and asymmetry parameter against $|\lambda_c|^2$ is presented. As in our analysis in Section 5.3 for $s \to dZ^*$, $|\lambda_c|^2$ is allowed to vary from 0.03 to 0.05, and $\mathrm{Re}(\lambda_u \lambda_c^*)$ is made to depend on $|\lambda_c|^2$ through the relation $\mathrm{Re}(\lambda_u \lambda_c^*) = -\sqrt{|\lambda_c|^2 |\lambda_u|^2 - J^2}$. These variations are displayed in Figs. 5.13 and 5.14 respectively.

It is noted that the variations of the decay rate and asymmetry parameter with $|\lambda_c|^2$ for $Z^0 \to s\bar{d}, \bar{s}d$ behave in a similar manner as in $s \to dZ^*$, $\bar{s} \to \bar{d}Z^*$. Steep variation of asymmetry parameter and decay rate against $|\lambda_c|^2$ are displayed, where the extremums occur at $|\lambda_c|^2 = 0.046$. When the decay rate decreases to its minimum, the asymmetry parameter increases to its maximum. Within the range of variation of $|\lambda_c|^2$, the decay rate vary from $\sim 3.5 \times 10^{-12}$ to $\sim 2 \times 10^{-8}$ GeV, whereas the magnitude of the asymmetry parameter may vary as much as 3 orders in magnitude, ranging from $\sim 1 \times 10^{-5}$ to $\sim 5 \times 10^{-2}$. We note here again that the sharp maximum displayed by $|a|$ versus $|\lambda_c|^2$ is because the decay rate encounters a sharp drop by 4 orders of magnitude at this point.

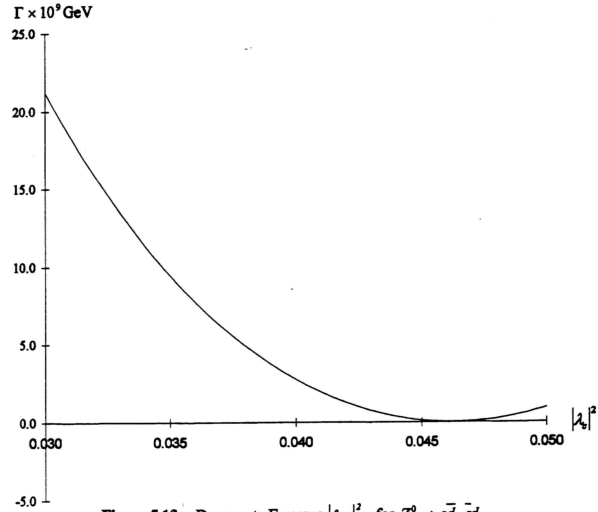

Figure 5.13. Decay rate Γ versus $|\lambda_e|^2$ for $Z^0 \to s\bar{d}, \bar{s}d$.

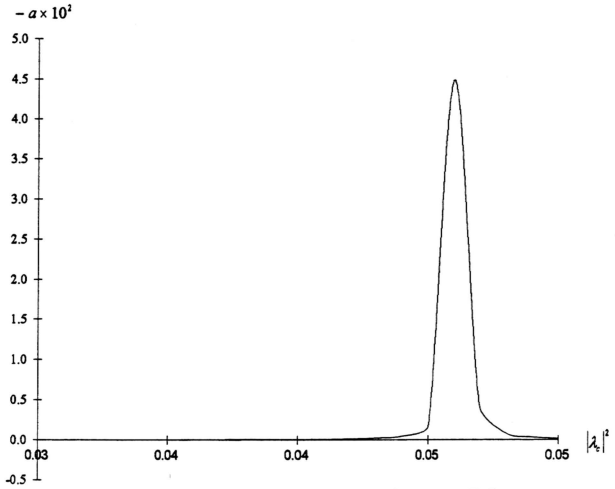

Figure 5.14. Asymmetry parameter a versus $|\lambda_c|^2$ for $Z^0 \to s\bar{d}, \bar{s}d$.

II. The process $Z^0 \to b\bar{s}, \bar{b}s$

For this process, we ignore the contribution of $|\lambda_u|^2$ and $\mathrm{Re}(\lambda_u \lambda_c^*)$ due to their smallness compared to $|\lambda_c|^2$. We fix the value of $|\lambda_c|^2$ = 0.00153, and the decay rate and asymmetry parameters are found to be:

Decay asymmetry, a = -8.8061×10^{-6}

Decay rate, Γ = 1.8568×10^{-8} GeV.

Generally, the magnitude of asymmetry parameter for this process is smaller compared to $Z^0 \to s\bar{d}, \bar{s}d$ because the corresponding decay rate is larger.

III. The process $Z^0 \to b\bar{d}, \bar{b}d$

We shall analyse the KM matrix elements dependence of asymmetry parameter and decay rate for this process as in the way we analyse the $b \to dZ^*$, $\bar{b} \to \bar{d}Z^*$ processes in Section 5.3(III). The variations of decay rate and asymmetry parameter with $|\lambda_c|^2$ are shown in Figure 5.15 and 5.16 for the two extreme values of $\mathrm{Re}(\lambda_u \lambda_c^*) = \pm|\lambda_u||\lambda_c|$ while fixing $|\lambda_u|^2 = 9.72 \times 10^{-6}$.

The variations of the decay rate and the asymmetry parameter with $\mathrm{Re}(\lambda_u \lambda_c^*)$ is shown in Fig. 5.17 and Fig. 5.18 for $|\lambda_u|^2 = 9.72 \times 10^{-6}$ and $|\lambda_c|^2 = 6.66 \times 10^{-5}$. $\mathrm{Re}(\lambda_u \lambda_c^*)$ is set to range from -2.6×10^{-5} to 2.6×10^{-5}.

From Fig. 5.16, we find that the magnitude of asymmetry parameter is generally higher than that for $\mathrm{Re}(\lambda_u \lambda_c^*) = |\lambda_u||\lambda_c|$. The magnitude of a being highest when $|\lambda_c|^2$ is

lowest, where a for $\mathrm{Re}(\lambda_u\lambda_e^*)=-|\lambda_u||\lambda_e|$ is about 8.5 times higher than a for $\mathrm{Re}(\lambda_u\lambda_e^*)=|\lambda_u||\lambda_e|$. When $|\lambda_c|^2$ tends to the upper end at 10×10^{-5}, the difference between a for both $\mathrm{Re}(\lambda_u\lambda_e^*)=\pm|\lambda_u||\lambda_e|$ narrowed, where a for $\mathrm{Re}(\lambda_u\lambda_e^*)=-|\lambda_u||\lambda_e|$ is only about 3.6 times higher than a for $\mathrm{Re}(\lambda_u\lambda_e^*)=|\lambda_u||\lambda_e|$. Fig. 5.18 shows that a has a rather flat variation with respect to $\mathrm{Re}(\lambda_u\lambda_e^*)$. Generally, a ranges from $\sim-8.0\times10^{-5}$ to $\sim-2.5\times10^{-3}$, depending on the phase of $\mathrm{Re}(\lambda_u\lambda_e^*)$ and the value of $|\lambda_c|^2$.

We also find that the decay rate for $\mathrm{Re}(\lambda_u\lambda_e^*)=|\lambda_u||\lambda_e|$ is generally higher. The difference between the decay rates for both $\mathrm{Re}(\lambda_u\lambda_e^*)=\pm|\lambda_u||\lambda_e|$ are highest at the lower end of $|\lambda_c|^2$, where Γ for $\mathrm{Re}(\lambda_u\lambda_e^*)=|\lambda_u||\lambda_e|$ being about 13 times higher. The difference becomes narrow when $|\lambda_c|^2$ tends to the higher end at 10×10^{-5}, where Γ for $\mathrm{Re}(\lambda_u\lambda_e^*)=|\lambda_u||\lambda_e|$ is only ~3.6 times higher. Fig. 5.17 shows the variation of decay rate with respect to $\mathrm{Re}(\lambda_u\lambda_e^*)$, where the value for Γ being highest when $\mathrm{Re}(\lambda_u\lambda_e^*)$ is towards the negative extreme. Generally the decay rate lies between 6.7×10^{-11} to 2.1×10^{-9} GeV.

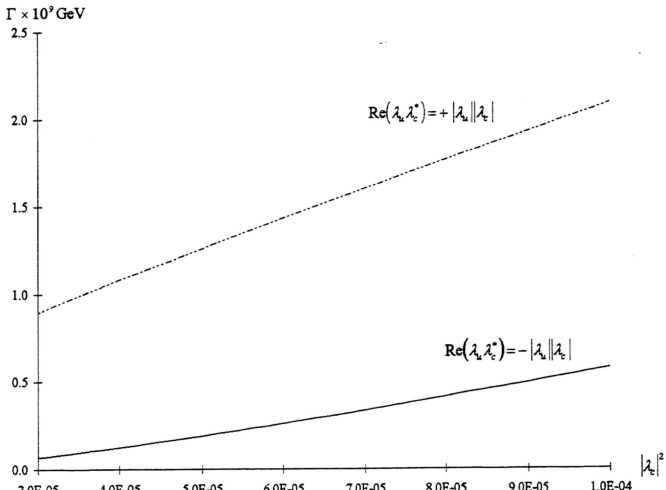

Figure 5.15. Decay rate Γ versus $|\lambda_c|^2$ for $Z^0 \to b\bar{d}, \bar{b}d$.

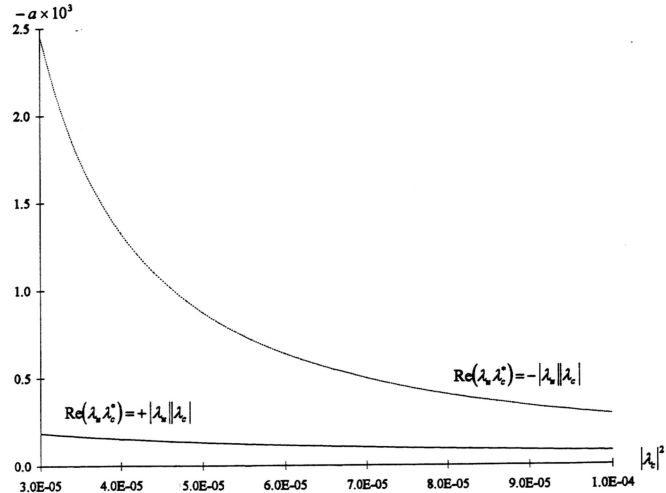

Figure 5.16. Asymmetry parameter a versus $|\lambda_c|^2$ for $Z^0 \to b\bar{d}, \bar{b}d$.

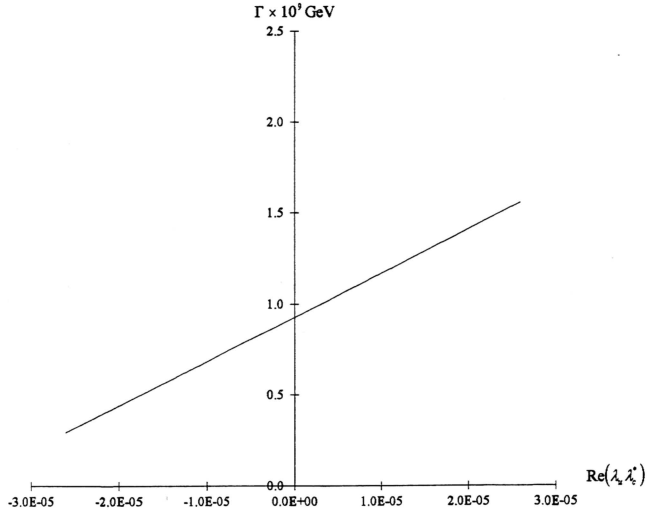

Figure 5.17. Decay rate Γ versus $\mathrm{Re}(\lambda_t \lambda_c^*)$ for $Z^0 \to b\bar{d}, \bar{b}d$.

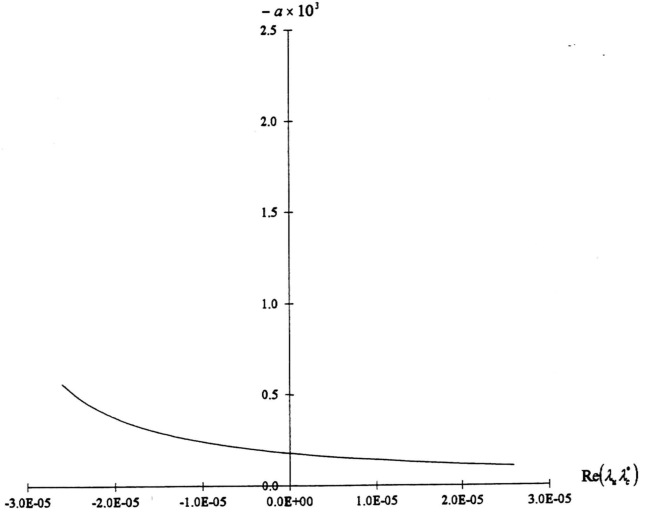

Figure 5.18. Asymmetry parameter a versus $\mathrm{Re}(\lambda_u \lambda_c^*)$ for $Z^0 \to b\bar{d}, \bar{b}d$.

Variations of the decay rates and asymmetry parameters with the KM matrix elements of flavour-changing Z^0 decays show similar behaviour to that displayed by flavour-changing quark transitions. Steep variations of decay asymmetry and decay rate against $|\lambda_c|^2$ are displayed in $Z^0 \to s\bar{d}$, $\bar{s}d$ decay, where they peaked at $|\lambda_c|^2 = 0.046$, as what happen in the case of $s \to d\,Z^*$ transition. Within the range of $|\lambda_c|^2$, a and Γ may vary as much as 3 to 4 orders in magnitude. Other processes show a rather flat variation with the KM matrix elements.

From Eqs. (5.45a) to (5.45f) we observe that

$$\tilde{f}_1 \approx M_Z^6,\ \tilde{f}_3 \approx M_Z^2 M_W^4,\ \tilde{f}_{13} \approx -M_Z^4 M_W^2 \tag{5.51}$$

are the dominant kinematic factors. The others, $\tilde{f}_2$, $\tilde{f}_{12}$ and $\tilde{f}_{23}$ are much smaller, by a factor of at least 300. The decay rate for $Z^0 \to \bar{q}_1 q_2$ is thus given approximately by

$$\begin{aligned}\Gamma \approx (3.026\text{keV})\Big\{&|\lambda_u|^2 |A_{ut} - C_{ut}|^2 + |\lambda_c|^2 |A_{ct} - C_{ct}|^2 \\ &+ 2\,\mathrm{Re}\left(\lambda_u \lambda_c^*\right)\mathrm{Re}\left(A_{ut} - C_{ut}\right)\left(A_{ct} - C_{ct}\right)^*\Big\}\end{aligned} \tag{5.52}$$

But the form factors at $k^2 = M_W^2$ are such that

$$A_{ut} - C_{ut} \approx A_{ct} - C_{ct} \tag{5.53}$$

The decay rate for $Z^0 \to \bar{q}_1 q_2$ is therefore

$$\Gamma \approx (3.026keV)|\lambda_t|^2 |A_{ct} - C_{ct}|^2 \tag{5.54}$$

In arriving at Eq. (5.54), we have utilized the unitarity condition of the KM matrix:

$$\lambda_u + \lambda_c + \lambda_t = 0 \tag{5.55}$$

A good knowledge of the relevant KM matrix elements allows us to predict the branching ratio of $Z^0 \to b\bar{s}$ from the Z-penguin to be 1.8×10^{-8}. The branching ratios for $Z^0 \to s\bar{d}$ and $Z^0 \to b\bar{d}$ cannot, however, be predicted with the same certainty, because of the

uncertain phases of the KM matrix elements involved. They are found of order (or less than) 10^{-9}.

To a good approximation, the asymmetry parameter for the flavour-changing decays of Z^0 arising from the Z-penguin is given by

$$\begin{aligned} a &\approx -2\left\{\mathrm{Im}\left(\lambda_u\lambda_c^*\right)/\left|\lambda_t^*\right|^2\right\}\mathrm{Im}\left\{\left(A_{ut}-C_{ut}\right)\left(A_{ct}^*-C_{ct}^*\right)\right\}/\left|A_{ut}-C_{ut}\right|^2 \\ &\approx -4.85\times10^{-4}\left(J/\left|\lambda_t^*\right|^2\right) \end{aligned} \tag{5.56}$$

For $Z^0\to b\bar{s}$, $a\sim-8.9\times10^{-6}$. For $Z^0\to s\bar{d}$ and $Z^0\to b\bar{d}$, the asymmetry parameter can be larger, of order $a\sim10^{-3}$ and 10^{-4} respectively, because of the smallness of the corresponding decay rates.

It is to be noted that a delicate cancellation is at work here, i. e. $A_{ut}-C_{ut}\approx A_{ct}-C_{ct}$. The active participation of A_j form factors in this subtle cancellation renders the asymmetry parameter to be very small.